With Eq. (7) the solution for $\{x\}$ is

$$\{x\}_{n,1} = [A^T]_{n,m} \left[[A]_{m,n} [A^T]_{n,m} \right]^{-1} \{y\}_{m,1} \tag{10}$$

Thus, the generalized inverse of $[A]_{m,n}$ for $m<n$ can be defined as

$$[A]^{+}_{n,m} = [A^T]_{n,m} \left[[A]_{m,n} [A^T]_{n,m} \right]^{-1} \tag{11}$$

It should be noted that

$$[A]_{m,n} \; [A]^{+}_{n,m} = [1]$$

However,

$$[A]^{+}_{n,m} \; [A]_{m,n} \neq [1]$$

Obviously Eq. (4) can also be considered as defining a generalized inverse. Thus the generalized inverse of $[A]_{m,n}$ for $m>n$ can be defined as

$$[A]^{+}_{n,m} = \left[[A^T]_{n,m} [A]_{m,n} \right]^{-1} [A^T]_{n,m} \tag{12}$$

Thus, the expression for $[A]^{+}_{n,m}$ depends on the relative magnitude of m and n. If $m=n$ both Eqs. (11) and (12) reduce to $[A]^{+} = [A]^{-1}$.

References

[1] Penrose, R., "A Generalized Inverse for Matrices," *Proceedings of the Cambridge Philosophical Society*, Vol. 51, 1955, pp. 406-413.

[2] Greville, T. N. E., "The Pseudoinverse of a Rectangular or Singular Matrix and Its Application to the Solution of Systems of Linear Equations," *SIAM Review*, Vol. 1, Jan. 1959, pp. 38-43.

[3] Cline, R. E., "Note on the Generalized Inverse of the Product of Matrices," *SIAM Review*, Vol. 6, Jan. 1964, pp. 57-58.

[4] Decell, H. P., Jr., "An Alternate Form of the Generalized Inverse of an Arbitrary Complex Matrix," *SIAM Review*, Vol. 7, July 1965, pp. 356-358.

[5] Decell, H. P., Jr., "An Application of the Cayley-Hamilton Theorem to Generalized Matrix Inversion," *SIAM Review*, Vol. 7, Oct. 1965, pp. 526-528.

[6] Söderström, T. and Stewart, G. W., "On the Numerical Properties of an Iterative Method for Computing the Moore-Penrose Generalized Inverse," *SIAM Journal of Numerical Analysis*, Vol. 11, March 1974, pp. 61-74.

[7] Decell, H. P., Jr., "A Special Form of a Generalized Inverse of an Arbitrary Complex Matrix," NASA TN D-2748, April 1965.

[8] Decell, H. P., "An Application of Generalized Matrix Inversion to Sequential Least Squares Parameter Estimation," NASA TN D-2830, May 1965.

Mach Reflection Using Ray-Shock Theory

Brian Edward Milton*

University of New South Wales, Kensington, N.S.W., Australia

Introduction

THE Mach reflection of shock waves at plane corners, as shown in Fig. 1, can be described by the three-shock theory (von Neumann)[1] or the ray-shock theory (Whitham).[2] The former gives the strength and direction of the Mach stem and reflected wave relative to the triple-point locus, and it may be used to locate the locus if the stem is assumed to be straight and normal to the wall. This assumption is inherent in the ray-shock approach, which uses the average strength of the Mach stem to determine its area and hence the triple-point position. Both theories, however, show noticeable deviation from experimental measurements of the triple-point locus position over the range of corner angles at which Mach reflection occurs. For simple corners, the three-shock theory is appropriate. However, for calculations of the shock front strength during repeated reflections in converging cavities of finite angle change or with curved walls, the ray-shock theory is more convenient and, in the latter case, is the only one to apply. Repeated applications of the theory to multiple reflections magnify errors occurring due to mislocation of the triple-point locus and an improvement in accuracy is therefore required. This has been achieved by modifying the area, Mach number (A, M) function used in the theory. Good agreement is now available in the range where the straight stem assumption conforms to reality.

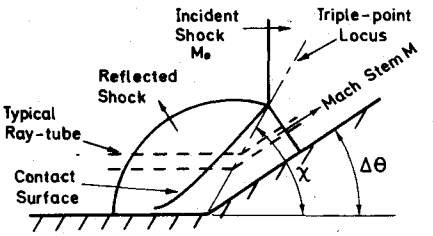

Fig. 1 Mach reflection configuration.

Area Change Function

The ray-shock theory consists of a set of equations based entirely on geometrical considerations which are related by the area change function first given by Chester.[3] This equation is usually written in the form

$$dA/A = -2M \, dM/K(M) \, (M^2-1) \tag{1}$$

where $K(M)$ is a monotonic function of M ranging from 0.5 for weak shocks to 0.394 for strong shocks. Integration of Eq. (1) has been carried out by Chisnell[4] to give the motion of a shock which is unaffected by disturbances from behind. A recent paper by Yousaf[5] shows that a more valid form of Eq. (1) for imploding shocks which includes interaction terms λ is

$$(dA/A) \, (1+\lambda) = -2M \, dM/K(M) \, (M^2-1) \tag{2}$$

His approach follows that of Whitham,[6] who derived Eq. (1) by examining the characteristics overtaking the shock. Alternative derivations are by Rosciszewski,[7] who integrated between neighboring characteristics, and Oshima et al,[8] who integrated along characteristics to obtain neglected correction terms.

Modified Area Change Function

Whitham's approach considers the flow equations in characteristic form

$$du + (dp/\rho a) + (ua/u+a) dA/A = 0 \text{ on } C^+ \tag{3a}$$

$$du - (dp/\rho a) + (ua/u-a) dA/A = 0 \text{ on } C^- \tag{3b}$$

Symbols p, ρ, a, and u are pressure, density, acoustic velocity, and velocity, respectively.

Substitution of the Rankine-Hugoniot conditions at the main shock front into the C^+ equation and subsequent manipulation give Eq. (1). This neglects interaction terms, as can be shown by an examination of the distance, time (x,t) plot of Fig. 2a. In the triangle $a\ b\ c$ formed by C^+ and C^- characteristics from point c away from the shock, which intersect the shock front line itself, terms on the C^- charac-

Received April 29, 1975.

Index category: Shock Waves and Detonations.

*Lecturer, School of Mechanical and Industrial Engineering.

teristic are individually zero if no disturbance exists upstream. Hence, an equation for the shock front of the same form as Eq. (3a) is equivalent to that of the C^+ characteristic.

The present approach obtains correction terms for the disturbed Mach reflection case by considering the triangle 1 2 3 shown on the x,t diagram of Fig. 2b. The line 1 2 is a small increment along the Mach stem immediately after reflection. Line 2 3 follows C^+ characteristics, but values along it differ from those given by the characteristic identity Eq. (3a) due to interactions of the reflected shock and the contact surface. Line 3 1 is not a characteristic, but connects an arbitrary point 3 in the region just prior to the formation of the reflected shock to point 1.

Terms on the shock front can be written as

$$(\mathrm{d}\zeta)_1^2 = (\mathrm{d}\zeta)_3^2 + (\mathrm{d}\zeta)_1^3 \tag{4}$$

where

$$\mathrm{d}\zeta = \mathrm{d}u + (\mathrm{d}p/\rho a) + (ua/u+a)\,\mathrm{d}(\ell\mathrm{n}A)$$

On line 3 1 the incident shock is undisturbed and $\mathrm{d}u$, $\mathrm{d}p$, and $\mathrm{d}(\ell\mathrm{n}A)$ are all zero, making $(\mathrm{d}\zeta)_1^3$ zero. To obtain values for the disturbance terms on line 3 2 the function $\mathrm{d}\zeta$ is assumed, as an approximation, to be continuous but is not, as mentioned above, equal to zero. By integrating between the end points and differentiating with respect to s in the characteristic direction, disturbance terms follow. Thus

$$\frac{\mathrm{d}}{\mathrm{d}s}\int_3^2 \mathrm{d}\zeta = \frac{\mathrm{d}\zeta_2}{\mathrm{d}s} - \frac{\mathrm{d}\zeta_3}{\mathrm{d}s} + \epsilon + \sigma \tag{5}$$

where

$$\epsilon = \int_3^2 \frac{\partial}{\partial s}\left(\frac{1}{\rho a}\right)\mathrm{d}p$$

and

$$\sigma = \int_3^2 \frac{\partial}{\partial s}\left(\frac{ua}{u+a}\right)\mathrm{d}(\ell\mathrm{n}A)$$

At either end of 23 the line represents a true characteristic and the characteristic identity holds, i.e., $\mathrm{d}\zeta_2/\mathrm{d}s$ and $\mathrm{d}\zeta_3/\mathrm{d}s$ equal zero. In the undisturbed case, $\mathrm{d}\zeta = 0$ holds for line 2 3 completely, and ϵ and σ also vanish. Substituting into Eq. (4) gives, for the disturbed case

$$(\mathrm{d}\zeta)_1^2 - (\epsilon+\sigma)\,\mathrm{d}s = 0 \tag{6}$$

Use of the Rankine-Hugoniot conditions on $(\mathrm{d}\zeta)_1^2$ now reduces Eq. (6) to Eq. (1) with additional correction terms, i.e.

$$\mathrm{d}(\ell\mathrm{n}A) = -\frac{2M\,\mathrm{d}M}{K(M)\,(M^2-1)} + \frac{(u_2+a_2)}{u_2 a_2}(\epsilon+\sigma)\,\mathrm{d}s \tag{7}$$

The correction terms ϵ and σ can be re-expressed as follows

$$\mathrm{d}\epsilon/\mathrm{d}p = (1/\rho a^2)\,(\partial a/\partial s) + (1/\rho^2 a)\,\partial\rho/\partial s \tag{8}$$

and

$$\mathrm{d}\sigma/\mathrm{d}(\ell\mathrm{n}A) = \{u^2\,(\partial a/\partial s) + a^2\,(\partial u/\partial s)\}/(u+a)^2 \tag{9}$$

These can be evaluated in the region upstream of the reflected shock and at the main front. A simplification is then made by using a trapezoidal integration between points 3 and 2, thus giving ϵ and σ. At point 3, $\partial a_3/\partial s$, $\partial p_3/\partial s$, and $\partial u_3/\partial s$ are all zero, making $(\mathrm{d}\epsilon/\mathrm{d}p)_3$ and $(\mathrm{d}\sigma/\mathrm{d}(\ell\mathrm{n}A))_3$ also zero. At 2 it has then been assumed that variations in the s direction can be approximated by variations in the shock front direction. Use has then been made of the "strong" shock equations for

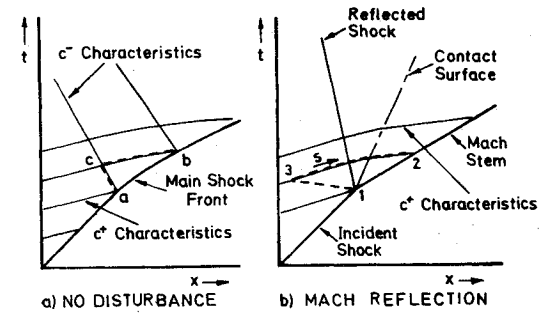

Fig. 2 $x-t$ **diagrams.**

evaluation purposes. The solution is

$$\left[\frac{\mathrm{d}\epsilon}{\mathrm{d}p}\right]_2 = -\left[\frac{\gamma-1}{\gamma}\right]^{1/2}\frac{1}{\rho_0 a_0 M^2}\frac{\mathrm{d}M}{\mathrm{d}s} \tag{10}$$

and

$$\left[\frac{\mathrm{d}\sigma}{\mathrm{d}(\ell\mathrm{n}A)}\right]_2 = \frac{4}{(\gamma+1)} \times \frac{[2\gamma(\gamma-1)]^{1/2}+\gamma(\gamma-1)}{\{[2\gamma(\gamma-1)]^{1/2}+2\}^2}\,a_0\frac{\mathrm{d}M}{\mathrm{d}s} \tag{11}$$

where subscript 0 refers to conditions ahead of the main shock wave. Correction terms then becomes

$$\epsilon = -\tfrac{1}{2}\left[\frac{\gamma-1}{2\gamma}\right]^{1/2}\frac{1}{\rho_0 a_0 M^2}(p_2-p_3)\frac{\mathrm{d}M}{\mathrm{d}s} \tag{12}$$

and

$$\sigma = \frac{2}{\gamma+1}\,\frac{[2\gamma(\gamma-1)]^{1/2}+\gamma(\gamma-1)}{\{[2\gamma(\gamma-1)]^{1/2}+2\}^2}\,a_0 \times \ell\mathrm{n}\left(\frac{A_2}{A_3}\right)\frac{\mathrm{d}M}{\mathrm{d}s} \tag{13}$$

Replacing A_2 and A_3, respectively, by the area of the Mach stem A, and the equivalent area of the upstream ray-tube A_0, and substituting the relations

$$\frac{a_2+u_2}{a_2 u_2} = \frac{\gamma+1}{a_0 M}\,\frac{[2\gamma(\gamma-1)]^{1/2}+2}{2[2\gamma(\gamma-1)]^{1/2}} \tag{14}$$

and

$$(p_2-p_3)/p_0 = (2\gamma/\gamma+1)\,(M^2-M_0^2) \tag{15}$$

gives

$$\left(\frac{a_2+u_2}{a_2 u_2}\right)(\epsilon+\sigma) = -\frac{1}{2\gamma}\left\{\left[\frac{\gamma(\gamma-1)}{2}\right]^{1/2}+1\right\} \times \left\{1-\frac{M_0^2}{M^2}\right\}\frac{\mathrm{d}M}{M\mathrm{d}s} - \frac{1}{2M}\ell\mathrm{n}\left(\frac{A_0}{A}\right)\frac{\mathrm{d}M}{\mathrm{d}s} \tag{16}$$

Then, by substitution into Eq. (7), the area change function follows, i.e.

$$\frac{\mathrm{d}A}{A} = -\left\{\frac{2M}{K(M)\,(M^2-1)} + \frac{\eta}{M}\right\}\mathrm{d}M \tag{17}$$

where $K(M)$ is that given by Whitham[6]; and

$$\eta = \frac{1}{2\gamma}\left\{\left[\frac{\gamma(\gamma-1)}{2}\right]^{1/2}+1\right\}\left\{1-\frac{M_0^2}{M^2}\right\}+\tfrac{1}{2}\ell\mathrm{n}\frac{A_0}{A} \tag{18}$$

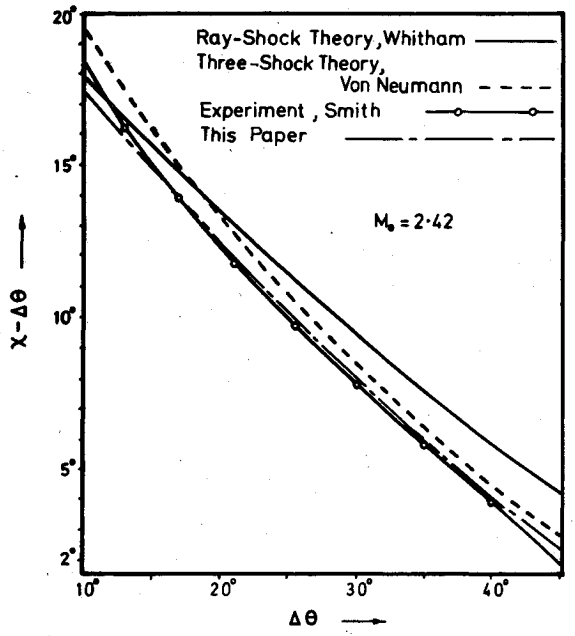

Fig. 3 Mach reflection for $M_0 = 2.42$.

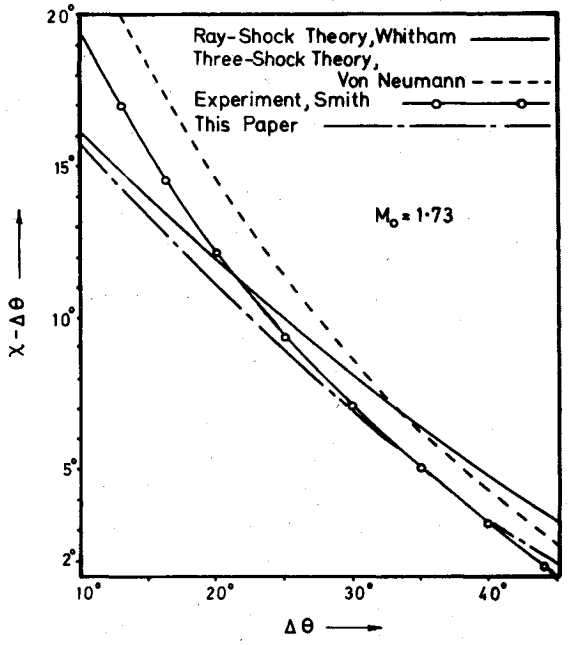

Fig. 4 Mach reflection for $M_0 = 1.73$.

For $\gamma = 1.4$

$$\eta = 0.546[1 - (M_0^2/M^2)] + \tfrac{1}{2}\ln A_0/A \qquad (19)$$

At glancing incidence, $M = M_0$ and $A = A_0$, making $\eta = 0$ and reducing Eq. (17) to Eq. (1).

Comparison of Theory and Experiment

Equation (17) has been used in combination with the normal ray-shock kinematic equations to obtain new results for the Mach reflection geometry. These are presented in Figs. 3 and 4 for incident shock Mach numbers 2.42 and 1.73. Comparisons are made in each case with the normal ray-shock theory, the three-shock theory, and experiment (Smith).[9] At the highest experimental Mach number, good agreement exists between the present method and Smith's experiments for the range of corner angles $14° < \Delta\theta < 40°$. At the lower corner angles the experimental curve deviates upwards, as would be expected from the observed appearance at low $\Delta\theta$ values of noticeable stem curvature. As $\Delta\theta$ approaches 45°, the curves again separate because the ray-shock theory continues to predict Mach reflection above values where regular reflection is known to occur.

As the incident Mach number is lowered, the range of agreement, although markedly improved over the unmodified ray-shock theory and the three-shock theory, becomes smaller. This is because the stem curvature becomes more noticeable with reduced strength. At a shock strength of $M_0 = 1.73$ the range of good agreement has reduced to $30° < \Delta\theta < 40°$. Other comparisons at $M_0 = 2.10$ and 1.51 show very close agreement in the ranges $20° < \Delta\theta < 40°$ and $30° < \theta < 37°$, respectively.

It should be noted that correction terms have been evaluated using strong shock equations for the shock front. A more accurate value for η should be obtained by using the exact equations. However, in view of the accuracy of the results, this extra complexity does not seem necessary.

References

[1] Von Neumann, J., "Theory of Shock Waves," *Collected Works*, Vol. VI, Pergamon Press, N.Y., 1963, pp. 238-299.

[2] Whitham, G. B., "A New Approach to Problems of Shock Dynamics, Part 1, Two-Dimensional Problems," *Journal of Fluid Mechanics*, Vol. 2, March 1957, pp. 145-171.

[3] Chester, W., "The Quasi Cylindrical Shock Tube," *Philosophical Magazine*, Vol. 45, Dec. 1954, pp. 1293-1301.

[4] Chisnell, R. F., "The Motion of a Shock Wave in a Channel with Applications to Cylindrical and Spherical Shock Waves," *Journal of Fluid Mechanics*, Vol. 2, May 1957, pp. 286-298.

[5] Yousaf, M., "The Effect of Overtaking Disturbances on the Motion of Converging Shock Waves," *Journal of Fluid Mechanics*, Vol. 66, Nov. 1974, pp. 577-591.

[6] Whitham, G. B., "On the Propagation of Shock Waves through Regions of Non-Uniform Area or Flow," *Journal of Fluid Mechanics*, Vol. 4, Aug. 1958, pp. 337-360.

[7] Rosciszewski, J., "Calculations of the Motion of Non-Uniform Shock Waves," *Journal of Fluid Mechanics*, Vol. 8, July 1960, pp. 337-367.

[8] Oshima, K., Sugaya, K., Yamamoto, M., and Totoki, T., "Diffraction of a Plane Shock Wave around a Corner," Rept. No. 393, Jan. 1965, Institute of Space and Aeronautical Science, Univ. of Tokyo.

[9] Smith, L. G., "Photographic Investigation of the Reflection of Plane Shocks in Air," Rept. 6271, Nov. 1945, Office of Scientific Research and Development.

Motion of a Stretched Cable with Small Curvature Carrying and Accelerating Mass

M. J. Forrestal,* D. C. Bickel,† and M. J. Sagartz‡
Sandia Laboratories, Albuquerque, N. Mex.

ROCKET-POWERED trolleys traveling along an aerial cable are used to simulate aircraft flight for the evaluation of airborne equipment at Sandia Laboratories, Albuquerque. The 1465 m long, 35 mm diameter steel cable is suspended between two mountain peaks. A winch positions the cable to heights up to 220 m above the canyon floor by tensioning up to 490 kN. At this tension, maximum sag is 30

Received June 16, 1975. This work was supported by the U.S. Energy Research and Development Administration.

Index category: Structural Dynamic Analysis.

*Division Supervisor, Shock Simulation Department. Associate Fellow AIAA.

†Division Supervisor, Shock Simulation Department.

‡Staff Member, Shock Simulation Department.